

Elastic DCS for $e + \text{CH}_4$ collisions, 1.5–100 eV

L Boesten† and H Tanaka‡

† Faculty of Science and Technology, Department of Physics, Sophia University, Chiyoda-ku, Kioicho 7, Tokyo 102, Japan

‡ Faculty of Science and Technology, Department of General Sciences, Sophia University, Chiyoda-ku, Kioicho 7, Tokyo 102, Japan

Received 18 September 1990, in final form 13 November 1990

Abstract. Absolute differential, integral and momentum transfer cross sections for electron–methane collisions were determined using a crossed beam spectrometer for impact energies from 1.5–100 eV and angles from 10° – 130° . Comparison with published total cross sections shows good agreement. At the shape resonance (7.5 eV) excitation measurements of the two vibrational peaks were taken and the angular distribution of their DCS was determined. The elastic DCS are compared with recent measurements and theoretical calculations.

1. Introduction

In recent years, the new technologies of plasma deposition of amorphous thin carbon films (Kline *et al* 1989) and plasma synthesis of diamonds (Mitsuda *et al* 1987) have revived interest in methane–electron collisions. Also, methane is one of the greenhouse gases whose oxidation chain in the troposphere includes CO_2 (Zellner *et al* 1989). Finally, because of its simple structure methane constitutes one of the few testing grounds for new theories on electron–molecule collisions. All of these require a detailed knowledge of the various cross sections of CH_4 .

In 1982, we published a fairly comprehensive set of elastic DCS for electron scattering from CH_4 for input energies from 3–20 eV over scattering angles from 30° – 140° (Tanaka *et al* 1982). This paper was thereafter referred to quite frequently either in DCS related measurements (Vušković *et al* 1983, Müller *et al* 1985, Curry *et al* 1985, Sohn *et al* 1986, Sakae *et al* 1989, Shyn *et al* 1990), in total cross section measurements (Jones 1985, Ferch *et al* 1985, Floeder *et al* 1985, Ohmori *et al* 1986, Lohmann *et al* 1986, Sueoka *et al* 1986, Dababneh *et al* 1988) or in theoretical work (Abusalbi *et al* 1983, Bloor *et al* 1986, Gianturco *et al* 1987, Gianturco and Scialla 1987, Jain 1986, Jain *et al* 1989, Lima *et al* 1985, 1989, Yuan 1988). Some papers even used our DCS to calibrate their measurements (Vušković *et al* 1983, Tanaka *et al* 1983, Curry *et al* 1985). However, compared to direct measurements of the total cross sections our estimates seemed to fall systematically short by about 30–35%. We have therefore remeasured the elastic DCS with a new spectrometer for impact energies from 1.5–100 eV and scattering angles from $(10)20^\circ$ – 130° , and obtained integrated and momentum transfer cross sections over the whole range. They are now in much better agreement with recent total cross section measurements. It is hoped that the same applies to the differential cross sections themselves. An independent continuation of the DCS measurements up to 700 eV has been published by Sakae *et al* (1989).

2. Apparatus and operating procedures

Our apparatus has been described in detail previously (Tanaka *et al* 1988). It is of the crossed electron and molecular beam type with a single 180° monochromator and a single 180° energy analyser both of mean radius 44 mm, and computer driven electron lenses. Overall resolution is 30–35 meV at all energies which is insufficient to resolve rotational excitations. Here, we discuss only a few points which we feel have not received sufficient attention in parallel work including our own (Tanaka *et al* 1982, Müller *et al* 1985, Sohn *et al* 1986, Shyn *et al* 1990).

(i) The magnetic field in the collision region *and the energy analyser* was reduced to less than 1 mG (2 mm permalloy shield plus Helmholtz coils). The low-energy regions of our apparatus, from gun to nozzle, nozzle to first accelerating lens, *and the path in the 180° energy analyser* (1–2 eV passing energy) have a total length of 220 mm. With such a long path even a uniform field of only 1 mG (10^{-7} T) deflects an electron beam of 1 eV energy by about 0.72 mm which roughly corresponds to the width of our virtual apertures. We have therefore reduced the remnant field of the permalloy shell by ‘fine-tuning’ with a pair of external Helmholtz coils and verifying the independence of the electron beam current from impact energy.

(ii) In a careful series of papers, Olander *et al* (1970), Jones *et al* (1969) and Brinkman *et al* (1981) have demonstrated that density and shape variations in the gas beam, and consequently changes in the observed DCS, occur when the Knudsen number is not held constant. A simple transmission check with He gas without pressure adjustments (ratio of Knudsen numbers: 64(He):17.3(CH₄)) neglects these density differences so that calibration by reference to He DCS may go astray. Furthermore, at low energies a careful alignment of gas beam and widened (!) electron beam is crucial in order to avoid angular distortions in the DCS.

(iii) The observed DCS and excitations of methane were normalized *point by point* with the help of simultaneous measurements of the DCS of He. These in turn were referred to known reliable He DCS. Our reference consists of the theoretical/experimental cross sections of Nesbet (1979) and Andrick *et al* (1975) up to 18 eV, and the measurements of Register *et al* (1980) joined and smoothed by a set of rational functions (Boesten 1988). Shyn’s He DCS (1980) deviate from this set by up to 20–50% depending on impact energy.

(iv) As our fittings indicate the observed lowest-angle DCS are probably somewhat too small. At these angles electrons from the tail of the beam can enter the analyser and contribute to background noise. We surmise that slight changes in space charge at the different pressures of He and CH₄ modify the width of the electron beam and cannot be fully compensated for by the relative flow method. Outliers at the lowest angle measurements have thus been excluded from the fits.

3. Fitting and integration methods

The measured elastic DCS were extrapolated with the help of three fitting methods and then integrated numerically. The fitting formulas can be described in a single expression as

$$\begin{aligned} d\sigma(\theta)/d\Omega &= |f(\theta)|^2 \\ 2ikf(\theta) &= N(k) \left\{ \sum_{l=0}^L [S_l(k) - 1](2l+1)P_l(\cos \theta) + C_L(\theta) \right\} \end{aligned}$$

$$C_L(\theta) = 2i\pi\alpha k^2 \left[\frac{1}{3} - \frac{1}{2} \sin(\theta/2) - \sum_{l=1}^L P_l(\cos \theta) / \{(2l+3)(2l-1)\} \right]$$

where C_L is the Born approximation of the higher phases in the Thompson form (Thompson 1966), k is the wavenumber of the free electron, α the atomic/molecular polarizability, P_l are the Legendre polynomials and $f(\theta)$ is the scattering amplitude. $S_l(k)$ is the scattering function, further details of which are given below. All quantities are expressed in atomic units. The use of this formula assumes that the highly symmetrical configuration of CH₄ allows the adaptation of a central field theory. The χ^2 -fittings follow the well known Boyden-Fletcher-Goldfarb-Fannon algorithm (Tone 1981, Press *et al* 1986).

In *simple phaseshift fitting* (abbreviated as (si), cf Andrick *et al* 1975), $N(k) \equiv 1$, and the scattering function becomes $S_l(k) = \exp\{2i\delta_l\}$ where δ_l are the usual phaseshifts. The cutoff parameter L is selected as small as compatible with a given (noisy) data set. Simple phaseshift fittings have been performed only up to 5 eV. The corresponding integrated cross sections are close to those of modified phaseshift fittings but their shapes deviate further from the experimental data.

In *modified phaseshift fitting* (md), (Register *et al* 1980, Tanaka *et al* 1982), $N(k)$ becomes a size parameter which also multiplies into C_L , and thus differs from δ_0 . The introduction of $N(k)$ dilutes the physical meaning of all phases and care is needed when comparing (md) phases with (si) phases (Sohn *et al* 1986). Also note that (md)

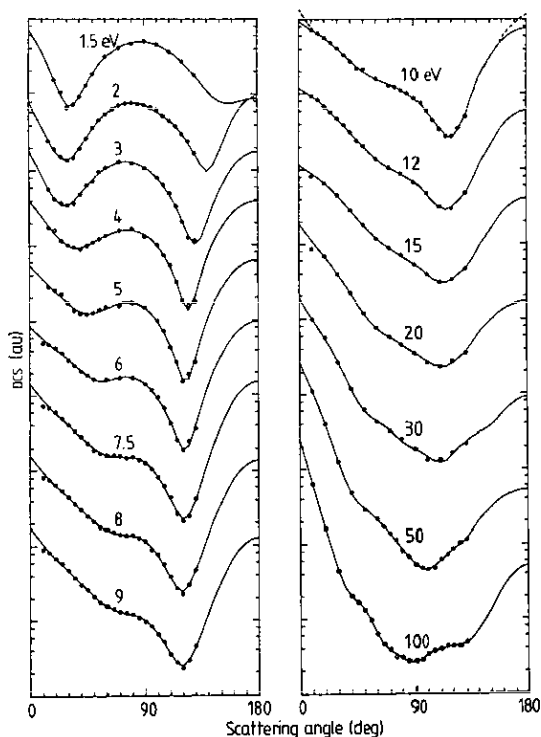


Figure 1. Measured elastic DCS (circles) and phaseshift fittings (full curves). Inelastic phaseshift fittings are used from 10 eV onwards; the broken curves in the tails of 10 eV show the tails of modified phaseshift fitting. For numerical values see table 1.

fits are invariant under transformations $\delta \rightarrow \delta \pm \pi$. Modified phaseshift fitting becomes difficult at 12–15 eV and fails beyond 20 eV.

Inelastic scattering in central fields (in) can be treated by the introduction of a complex potential which in turn necessitates a reformulation of the scattering function as $S_l(k) = \beta_l \exp(2i\delta_l)$ (Mott *et al* 1965, Bransden 1970), $N(k) \equiv 1$. Here β is the 'inelasticity', a real number. In the present paper we have assumed additionally that the higher phaseshifts can be expressed by the traditional Born approximation $C_L(\theta)$. Inelastic phaseshift fits were used from 10 eV onwards. Occasionally, we had to add, temporarily, an artificial data point at 180° to obtain a reasonable set of initial parameters, however, these points were removed before the final fitting.

For all energies beyond 2 eV, two or more sets of fitting parameters were found. The final fits were selected according to (a) the speed of convergence (quadratic . . .); (b) the size of χ^2 ; (c) the shape beyond 130° ; and (d) a smooth behaviour of the integrated and momentum transfer cross sections σ_I and σ_M . The latter comes close to a two-dimensional fitting in DCS- θ and DCS-eV space. The (md) and (in) fits connect smoothly at 10 eV except for small changes in the extreme tails, cf figure 1. At higher

Table 1. Elastic cross sections in units of $10^{-16} \text{ cm}^2 \text{ sr}^{-1}$ and 10^{-16} cm^2

θ	E_0 (eV)							
	1.5	2	3	4	5	6	7.5	8
10						5.101	7.360	8.127
15		0.250	0.562	1.753	2.810	4.909	6.862	7.517
20	0.151	0.194	0.419	1.604	2.532	4.390	6.000	6.432
25	0.102	0.152	0.368	1.158	2.247	3.765	4.942	5.407
30	0.064	0.136	0.347	1.014	1.734	3.009	4.078	4.431
35	0.070	0.147	0.364	0.948	1.383	2.546	3.396	3.622
40	0.089	0.195	0.480	0.895	1.262	2.139	2.859	3.016
45	0.126	0.266	0.635	0.992	1.232	1.889	2.315	2.466
50	0.181	0.367	0.722	1.102	1.283	1.661	1.879	2.076
55		0.465	0.953	1.217	1.416		1.706	1.765
60	0.312	0.555	1.092	1.357	1.540	1.653	1.609	1.643
65		0.645					1.591	1.517
70	0.412	0.718	1.306	1.595	1.588	1.725	1.574	1.409
75		0.758					1.484	1.382
80	0.471	0.771	1.246	1.673	1.737	1.733	1.528	1.403
85		0.748					1.387	1.271
90	0.505	0.722	1.082	1.313	1.530	1.421	1.255	1.153
95		0.677				1.190	1.050	0.879
100	0.458	0.625	0.804	1.016	1.001	0.945	0.816	0.773
105		0.528	0.640	0.738	0.734	0.680	0.612	0.568
110	0.363	0.451	0.492	0.543	0.444	0.419	0.435	0.387
115		0.380	0.332	0.323	0.282	0.257	0.262	0.273
120	0.272	0.302	0.206	0.183	0.153	0.189	0.209	0.227
125		0.239	0.126	0.160	0.192	0.249	0.245	0.303
130	0.175	0.167	0.115	0.179	0.281	0.356	0.414	0.474
σ_I	3.61	5.61	9.25	14.41	18.04	22.97	26.49	26.30
σ_M	3.49	5.40	8.43	13.71	17.55	21.79	25.07	23.76
L	6	6	6	5	6	6	7	7
χ^2	0.10	0.22	0.50	1.24	2.22	0.92	1.00	0.81

Table 1. (continued)

θ	E_0 (eV)							
	9	10	12	15	20	30	50	100
10	8.991	7.237	9.287	8.143	8.612	9.858	11.046	6.3156
15	8.225	6.485	8.308					
20	6.861	5.646	6.764	6.659	6.905	5.596	4.0244	1.6226
25	5.853	4.885	5.789					
30	4.713	4.107	4.784	4.555	3.956	2.600	1.2737	0.4393
35	3.786	3.361	3.937					
40	3.045	2.741	3.122	2.866	2.213	1.153	0.4923	0.2047
45	2.609	2.206	2.395					0.1664
50	2.126	2.142	2.021	1.803	1.206	0.606	0.2897	0.1302
55	1.771							0.0967
60	1.566	1.570	1.364	1.176	0.768	0.415	0.2174	0.0623
65	1.430						0.1702	0.0460
70	1.308	1.254	1.034	0.879	0.586	0.317	0.1393	0.0386
75	1.273	1.201					0.1141	0.0305
80	1.210	1.089	0.862	0.704	0.462	0.246	0.0818	0.0301
85	1.094	0.986					0.0685	0.0268
90	0.972	0.852	0.656	0.525	0.351	0.183	0.0528	0.0269
95	0.843	0.736					0.0480	0.0280
100	0.658	0.588	0.472	0.389	0.263	0.130	0.0464	0.0332
105	0.516	0.441					0.0484	0.0369
110	0.348	0.336	0.313	0.306	0.231	0.131	0.0623	0.0393
115	0.272	0.271					0.0722	0.0428
120	0.228	0.268	0.294	0.329	0.274	0.162	0.0860	0.0429
125	0.293	0.347					0.1032	0.0430
130	0.456	0.502	0.475	0.465	0.355	0.215	0.1164	0.0488
σ_I	25.55	23.02	20.74	18.27	14.41	9.49	6.57	3.20
σ_M	21.77	20.21	14.63	11.78	6.95	3.87	2.22	1.08
L	7	5	5	5	5	5	6	7
χ^2	0.76	0.67	1.08	0.56	0.37	2.52	0.14	0.10

impact energies our fits look similar to the measurements of Shyn *et al* (1990) up to 156°. Nevertheless, a careful inspection of figure 1 reveals inconsistencies in the tails. These fits are probably the first application of the inelastic phaseshift formula over a wider range of DCS (however, see Allen *et al* 1987 and Allen and McCarthy 1987 for a different approach; our attempts with their formulas produced only 'chance hits' in a multiparameter space divided by steep crevices).

Integral σ_I and momentum transfer cross sections σ_M were obtained by numerical integration under the fits. Cutoff parameter L and χ^2 are shown in the lowest rows of table 1, but note that χ^2 is based on the arbitrary assumption that the measurement errors are of size $0.05\sqrt{y}$ where y is the number of counts observed.

4. Results and discussion

Table 1 gives the measured DCS and the integrated cross sections. Figure 1 shows the quality of the fits obtained. In figure 2 we compare our integrated cross sections with

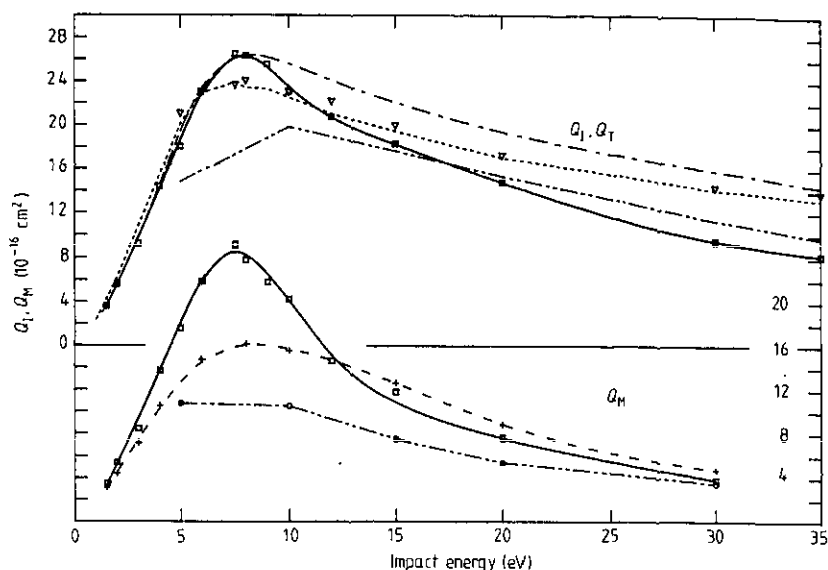


Figure 2. Integrated elastic and momentum transfer cross sections Q_I and Q_M in comparison with other work. Full curve and squares, this work; ---, Q_T Jones (1985); ····, Q_T Sueoka *et al* (1986) (connected by straight lines); -·-·-·, Q_I Shyn (1990) and Q_M (connected by straight lines); triangles, Q_T Floeder *et al* (1985); ---, Q_M Davies *et al* (1989).

recent measurements of the total cross sections Q_T , and figure 3 illustrates the broad resonance shape at 7.5 eV. Error estimates have been discussed previously (Tanaka *et al* 1982); the present measurements are presumed to be correct to about $\pm 15\%$. Comparison with other experimental work (Sohn *et al* 1986, Rohr 1986, Shyn *et al* 1990) is shown in figure 4. There are several features worth mentioning.

(a) Figure 1, 10 eV shows the smooth transition between the two fitting methods (md) and (si). (md) fittings at higher energies either produce extremely steep extensions with endpoints at 180° higher than the DCS at 0° or strong oscillations over the experimental data. The measurements and (si) fits of Sohn *et al* (1986) and Rohr (1986) for 1.5, 2 and 3 eV are smaller than our data and have a minimum at 37.5° while ours falls at 32° (1.5 eV, cf figure 4). Their integrated cross sections drop below the

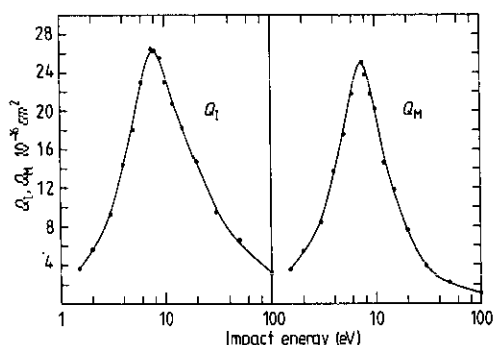


Figure 3. Integrated (Q_I) and momentum transfer cross sections (Q_M) as a function of impact energy.

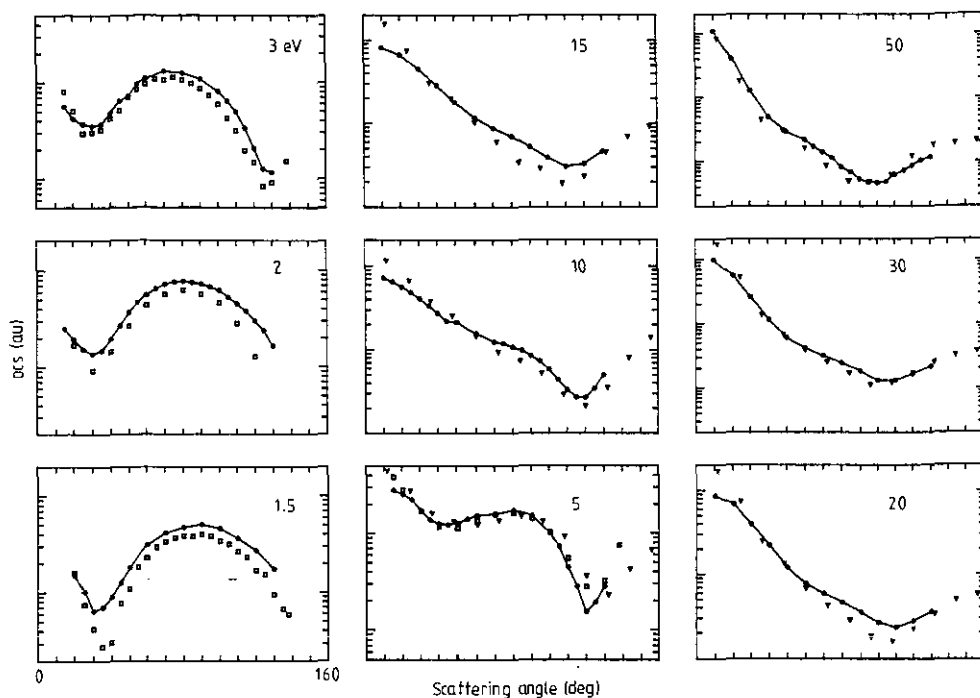


Figure 4. Comparison with other DCS measurements. Circles connected by straight lines, this work; squares, Sohn *et al* (1986) and Rohr (1980); triangles, Shyn (1990). Ordinates are correctly marked, for numerical values see table 1.

trend-line of figure 2. The DCS of Shyn *et al* (1990) approach our DCS in size and shape only approximately (note compressed scales). Their integrated cross sections deviate considerably from the main trend of figure 2.

(b) Low-angle plots of DCS against eV up to 30° (not shown) reveal a dip in the DCS of about 10–15% at 10 eV. A similar phenomenon has been observed in He and interpreted as due to the opening of inelastic channels (Wagenaar *et al* 1986).

(c) Most of the total cross sections Q_T of figure 2 have been measured by time-of-flight transmission methods. Neutral dissociation begins at 9 eV; the size of the corresponding contributions to Q_T can be estimated from figure 6 of Davies *et al* (1989) as $Q = 1.2/1.7/2.2 \times 10^{-16} \text{ cm}^2$ at 10/15/20 eV. Ionization starts at about 13 eV and reaches 10^{-16} cm^2 at 20 eV and $4.3 \times 10^{-16} \text{ cm}^2$ at 85 eV (Winters 1975, Nakamura 1990). When these processes are added to our integrated cross sections σ_1 , good over-all agreement with Q_T of Jones (1985) and Lohmann *et al* (1986) is obtained. Jones' measurements have quite recently been confirmed to high precision by Nishimura *et al* (1990). However, inclusion of the vibrational cross sections, $Q = 0.37/2.34/1.52/0.754 \times 10^{-16} \text{ cm}^2$ at 2/7.5/10/20 eV (Ohmori values as given by Davies *et al* 1989) raises the peak in the vicinity of 7.5 eV to a total of $28.3 \times 10^{-16} \text{ cm}^2$ which agrees quite closely with the direct measurements of Dababneh *et al* (1988), except that our σ_1 beyond 8 eV seems to drop somewhat faster than their σ_T . Note that Q_T derived from swarm experiments depends heavily on a correct estimation of the elastic DCS.

(d) The low-energy momentum transfer cross sections of Davies *et al* (1989) obtained from drift-velocity experiments are smaller than our estimates (~65% below

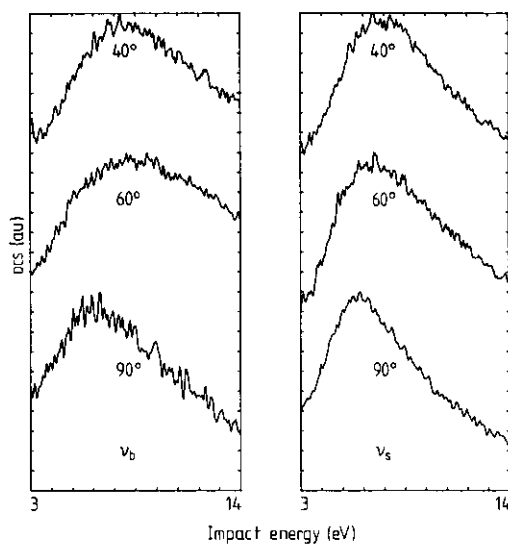


Figure 5. Excitation measurements of the two vibrational modes (bending ν_{24} and stretching ν_{13}) as function of impact energy for 40°, 60° and 90° scattering.

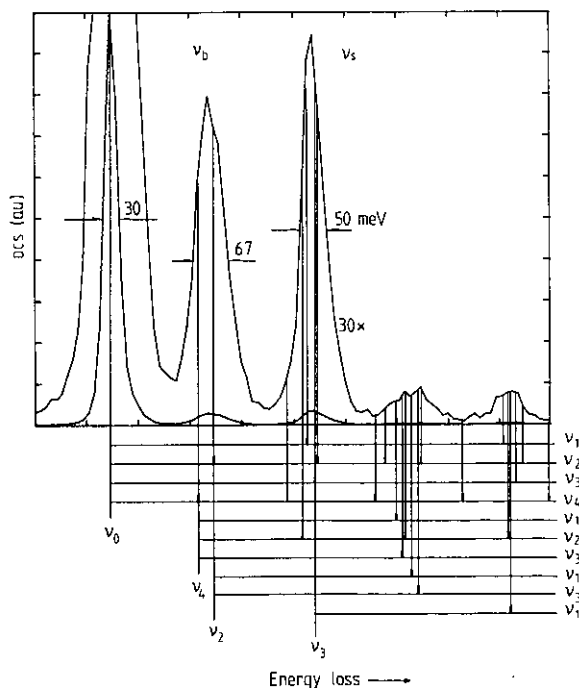


Figure 6. 90° energy-loss spectrum at resonance impact energy 7.5 eV. The four fundamental vibrational modes ($\nu_1 = 362$, $\nu_2 = 190$, $\nu_3 = 374$, $\nu_4 = 162$ meV) together with possible harmonics are indicated below the spectrum. Considerable rotational broadening shows up in the tails of the peaks.

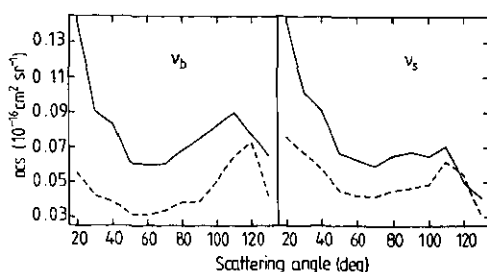


Figure 7. Vibrational DCS at 7.5 eV impact energy as a function of scattering angle. ---, determined by ± 10 meV integration; —, determined by valley-to-valley integration in figure 6, cf text.

12 eV) and tend towards 150% at larger energies, cf figure 2. Shyn's σ_I (Shyn *et al* 1990) is yet smaller (40% at 7.5 eV) but approaches our values at 30–50 eV. Estimates of σ_M are less certain than those of σ_I due to the larger influence of the extrapolated high-angle tail, nevertheless, the main contribution arises from the area under the measured values. Figure 3 suggests that the two peaks of σ_I and σ_M are nearly equal. Belatedly, a similar trend towards more equal peaks has appeared in Q_T plots of swarm experiments (Nakamura 1990, Tawara 1990) (20:17.5, ours 26.5:25.0).

(e) Figure 5 confirms the broad shape resonance at 7.5 eV by excitation measurements of the two vibrational compound peaks ν_{24} and ν_{13} . In addition to rotational widening (Müller *et al* 1985) the second peak also contains a large amount of harmonics, see figure 6. With methane we find that the peaks shift with increasing angles towards lower energies, in ethane they remain rather constant (Boesten *et al* 1990), while in silane an opposite trend toward higher energies was observed (Tanaka *et al* 1990).

Vibrational cross sections are put onto an absolute scale by comparison with the elastic peak, and often integration over a narrow interval, e.g. ± 10 meV, is used to reduce the noise. On the other hand, swarm experiments try to describe the total effect of the compound vibrational peaks in form of single functions of energy. According to this method the vibrational DCS should be obtained by a valley-to-valley integration under the traces of figure 6. In figure 7 we demonstrate that the two integration methods can differ by as much as 250%. Note that excitation measurements correspond to the peak values themselves. Their physical meaning is yet less clearly defined, see for example ν_b of figure 6.

5. Comparison with recent theories in the range 1.5–100 eV

In figure 8 we compare our fits with several recent theoretical DCS. Note that the fits represent our measurements in the range 10(20)–130° to within a few percent. The Ramsauer–Townsend minimum in the 2A_1 state is out of range. Here we are mostly interested in the broad resonance of the 2T_2 state and the over-all DCS behaviour up to 100 eV. There are several theoretical streams, (a) the Schwinger multichannel formulations of Lima *et al* (1985, 1989) with non-empirical polarization effects; (b) the one-centre potential descriptions of Gianturco *et al* (1987) and Gianturco and Scialla (1987) via parameter-free model interactions for static, exchange and polarization contributions, the one-centre spherical model with local exchange and model polarization potentials in combination with complex optical potentials of Jain (1986),

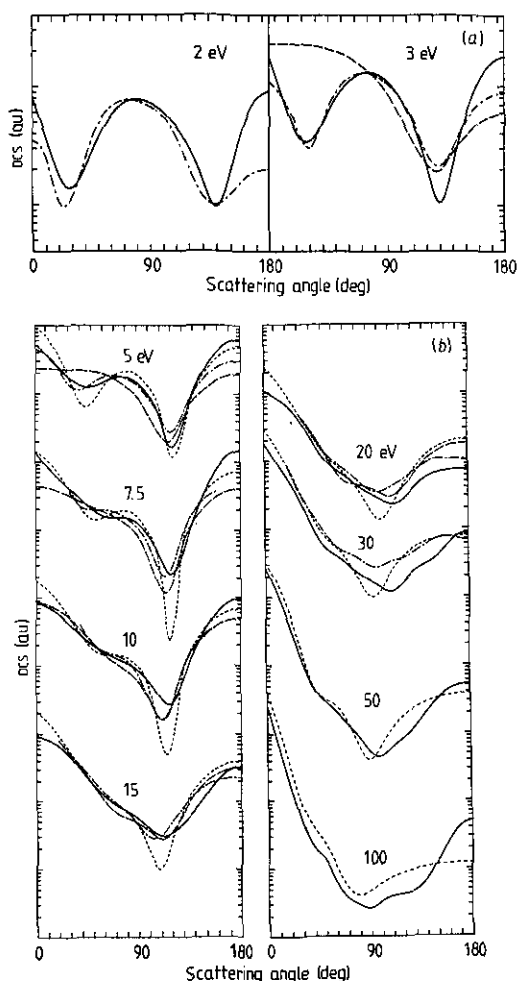


Figure 8. Comparison of measured elastic DCS (— phaseshift fits) with various theories for (a) 2 and 3 eV and (b) 5–100 eV. ---, Jain (1986) (SEPa-sets except 100 eV where we used his SEP-set); — · —, Bloor *et al* (1986); — — —, Lima *et al* (1985, 1989).

Jain *et al* (1989), and the modified exact static exchange calculations with spherical wavefunctions of Yuan (1988); (c) the complex Kohn variational method of McCurdy *et al* (1989); and (d) the parameter-free continuum multiple scattering models of Tossel *et al* (1984) and Bloor *et al* (1986). Good agreement is found between Bloor *et al* and our low-energy measurements up to 10 eV; our high-angle extensions though are steeper and the flat tail in their plot of 2 eV appears in our fits only at 1.5 eV. At low energies Jain's model agrees qualitatively with our measurements, but minima and maxima are exaggerated. At higher energies (where Jain's complex potential sets in) the minimum shifts away from that of the data. Also it looks as if our data and fits develop a second minimum at around 130° traces of which can be recognized in Bloom's $X\alpha$ -method. Lima's model fails at low energies, even with static exchange polarization approximations included. Gianturco's DCS at 8 and 10 eV (not shown) come close to our data while his plot of 4 eV deviates in shape from our experiments and the peak of his Q_T appears at 9 eV (Gianturco and Scialla 1987).

Yuan's total cross sections (1988, not shown) are the highest among all theories and experiments. Jain's integrated cross sections (1986) peak at 10 eV ($24.93 \times 10^{-16} \text{ cm}^2$) but then become larger than our estimates beyond 10 eV. There is no dip at 10 eV. His momentum cross sections reach a maximum of about $20 \times 10^{-16} \text{ cm}^2$ or 80% of our estimate. In view of the rather different shapes of the DCS, even agreement of this order is rather surprising; σ_1 and σ_M contain too little information to serve as a criterion for the evaluation of theories (McCurdy *et al* 1989).

6. Conclusion

We have provided a new revised set of elastic DCS and hope that they will serve as a reliable standard for future related work. Comparison with theory shows clearly the need for measurements extending to higher angles at least up to 150° . Such an instrument is now under construction.

References

- Abusalbi N, Eades R A, Nam T, Thirumalai D, Dixon D A and Truhlar D G 1983 *J. Chem. Phys.* **78** 1213–27
Allen L J, Brunger M J, McCarthy I E and Teubner P J O 1987 *J. Phys. B: At. Mol. Phys.* **20** 4861–8
Allen L J and McCarthy I E 1987 *Phys. Rev. A* **36** 2570–5 and references therein
Andrick D and Bitsch A 1975 *J. Phys. B: At. Mol. Phys.* **8** 393–410
Bloor J E and Sherrod R E 1986 *J. Phys. Chem.* **90** 5508–18
Boesten L and Tanaka H 1988 *43rd meeting of the Physical Soc. of Japan* 31a-G2-9 to be published
Boesten L, Tanaka H, Kubo M, Sato H, Kimura M, Dillon M A and Spence D 1990 *J. Phys. B: At. Mol. Opt. Phys.* **23** 1905–13
Bransden B H 1970 *Atomic Collision Theory* (New York: Benjamin) sect 1–5
Brinkmann R T and Trajmar S 1981 *J. Phys. E* **14** 245–55
Curry P J, Newell W R and Smith A C H 1985 *J. Phys. B: At. Mol. Phys.* **18** 2303–18
Dababneh M S, Hsieh Y-F, Kauppila W E, Kwan C K, Smith S J, Stein T S and Uddin M N 1988 *Phys. Rev. A* **38** 1207–16
Davies D K, Kline L E and Bies W E 1989 *J. Appl. Phys.* **65** 3311–23
Ferch J, Granitzka B and Raith W 1985 *J. Phys. B: At. Mol. Phys.* **18** L445–50
Floeder K, Fromme D, Raith W, Schwab A and Sinapius G 1985 *J. Phys. B: At. Mol. Phys.* **18** 3347–59
Gianturco F A, Jain A and Pantano L C 1987 *J. Phys. B: At. Mol. Phys.* **20** 571–86
Gianturco F A and Scialla S 1987 *J. Phys. B: At. Mol. Phys.* **20** 3171–89
Jain A 1986 *Phys. Rev. A* **34** 3707–22
Jain A, Weatherford C A, Thompson D G and McNaughten P 1989 *Phys. Rev. A* **40** 6730–3
Jones R H, Olander D R and Kruger V R 1969 *J. Appl. Phys.* **40** 4641–9
Jones R K 1985 *J. Chem. Phys.* **82** 5424–7
Kline L E, Partlow W D and Bies W E 1989 *J. Appl. Phys.* **65** 70–8
Lima M A P, Gibson T L, Huo W M and McKoy V 1985 *Phys. Rev. A* **32** 2696–701
Lima M A P, Watari K and McKoy V 1989 *Phys. Rev. A* **39** 4312–5
Lohmann B and Buckman S J 1986 *J. Phys. B: At. Mol. Phys.* **19** 2565–70
McCurdy C W, Rescigno T N 1989 *Phys. Rev. A* **39** 4487–93
Mitsuda Y, Kojima Y, Yoshida T and Akashi K 1987 *J. Mater. Sci.* **22** 1557–62
Mott N F and Massey H S W 1965 *The Theory of Atomic Collisions* 3rd edn (Oxford: Clarendon) ch VIII, 2.1
Müller R, Jung K, Kochem K-H, Sohn W and Ehrhardt H 1985 *J. Phys. B: At. Mol. Phys.* **18** 3971–85
Nakamura Y 1990 Private communication
Nesbet R K 1979 *Phys. Rev. A* **20** 58–70
Nishimura H and Sakae T 1990 *Japan J. Appl. Phys.* **29** 1372–6
Ohmori Y, Kitamori K, Shimozuma M and Tagashira H 1986 *J. Phys. D* **19** 437–55
Olander D R and Kruger V 1970 *J. Appl. Phys.* **41** 2769–76, 4388–91

- Press W H, Flannery B P, Teukolsky S A and Vetterling W T 1986 *Numerical Recipes* (Cambridge: Cambridge University Press) ch 10.7
- Register D F, Trajmar S and Srivastava S K 1980 *Phys. Rev. A* **21** 1134-51
- Rohr K 1980 *J. Phys. B: At. Mol. Phys.* **13** 4897-905
- Sakae T, Sumiyoshi S, Murakami E, Matsumoto Y, Ishibashi K and Katase A 1989 *J. Phys. B: At. Mol. Opt. Phys.* **22** 1385-94
- Shyn T W 1980 *Phys. Rev. A* **22** 916-22
- Shyn T W and Cravens T E 1990 *J. Phys. B: At. Mol. Opt. Phys.* **23** 293-300
- Sohn W, Kochem K-H, Scheuerlein K-M, Jung K and Ehrhardt H 1986 *J. Phys. B: At. Mol. Phys.* **19** 3625-32
- Suoeka O and Mori M 1986 *J. Phys. B: At. Mol. Phys.* **19** 4035-50
- Tanaka H, Boesten L, Matsunaga D and Kudo T 1988 *J. Phys. B: At. Mol. Opt. Phys.* **21** 1255-63
- Tanaka H, Boesten L, Sato H, Kimura M, Dillon M A and Spence D 1990 *J. Phys. B: At. Mol. Opt. Phys.* **23** 577-88
- Tanaka H, Kubo M, Onodera N and Suzuki A 1983 *J. Phys. B: At. Mol. Phys.* **16** 2861-9
- Tanaka H, Okada T, Boesten L, Suzuki T, Yamamoto T and Kubo M 1982 *J. Phys. B: At. Mol. Phys.* **15** 3305-19
- Tawara H, Itikawa Y, Nishimura H, Tanaka H and Nakamura Y 1990 Collision data involving Hydro-Carbon Molecules *Research Report NIFS-data Series no 6*, National Inst. for Fusion Science, Nagoya, Japan
- Thompson D G 1966 *Proc. R. Soc. A* **294** 160-74
- Tone K 1981 *Basic* (Tokyo: Baifukan) in Japanese
- Tossell J A and Davenport J W 1984 *J. Chem. Phys.* **80** 813-21
- Vušković L and Trajmar S 1983 *J. Chem. Phys.* **78** 4947-51
- Wagenaar R W, De Boer A, Van Tubergen T, Los J and De Heer F J 1986 *J. Phys. B: At. Mol. Phys.* **19** 3121-43
- Winters H F 1975 *J. Chem. Phys.* **63** 3462-6
- Yuan J 1988 *J. Phys. B: At. Mol. Opt. Phys.* **21** 3113-21
- Zellner R and Weibring G 1989 *Z. Phys. Chem.* **161** 167-88